Evaluation of Model Summertime Boundary Layer Cloud Development over Complex Terrain in New York State

LANXI MIN,[a,b] QILONG MIN,[b] AND YUYI DU[b]

[a] *School of Computer and Information Engineering, Xiamen University of Technology, Xiamen, Fujian, China*
[b] *Atmospheric Sciences Research Center, University at Albany, State University of New York, Albany, New York*

(Manuscript received 22 October 2021, in final form 20 June 2022)

ABSTRACT: Weather forecasting over complex terrain with diverse land cover is challenging. Utilizing the high-resolution observations from New York State Mesonet (NYSM), we are able to evaluate the surface processes of the Weather Research Forecast (WRF) Model in a detailed, scale-dependent manner. In the study, possible impacts of land–atmosphere interaction on surface meteorology and boundary layer cloud development are investigated with different model resolutions, land surface models (LSMs), and planetary boundary layer (PBL) physical parameterizations. The High-Resolution Rapid Refresh, version 3 (HRRR), forecasting model is used as a reference for the sensitivity evaluation. Results show that over complex terrain, the high-resolution simulations (1 km × 60 vertical levels) generally perform better compared to low-resolution (3 km × 50 levels) in both surface meteorology and cloud fields. LSMs play a more important role in surface meteorology compared to PBL schemes. The NoahMP land surface model exhibits daytime warmer and drier biases compared to the Rapid Update Cycle (RUC) due to better prediction of the Bowen ratio in RUC. The PBL schemes would affect the convective strength in the boundary layer. The Shin–Hong (SH) scale-aware scheme tends to produce the strongest convective strength in the PBL, while the ACM2 PBL scheme rarely resolved convection even at 1-km resolution. By considering the radiation effect of subgrid-scale (SGS) clouds, the Mellor–Yamada–Nakanishi–Niino eddy diffusivity mass flux (MYNN-EDMF) predicted the highest cloud coverage and lowest surface solar radiation bias. The configuration of SGS clouds in MYNN-EDMF would not only significantly reduce shortwave radiation bias, but also affect the convection behaviors through land surface–cloud–radiation interaction.

KEYWORDS: Complex terrain; Boundary layer; Cumulus clouds; In situ atmospheric observations; Short-range prediction; Model evaluation/performance

1. Introduction

Boundary layer clouds (BLCs) play an important role in radiative forcing and modulation of near surface and mixed layer thermodynamic properties (Stull 1988), the seasonal and diurnal patterns of which also influence vegetation growth (Freedman et al. 2001; Min 2005). Simulation of BLCs is important for the forecasting of local weather and climate (Bélair et al. 2004; Berg et al. 2013). Accurate prediction of the diurnal cycle of BLCs will also result in the better short-term forecast of solar radiation. The forecasting of fair-weather cumulus fields is essential for the renewable energy generation. With passage of cumulus clouds, the solar energy produced by a photovoltaic (PV) site can drop as much as 70% from clear-sky value (Miller et al. 2017; Manning and Baldick 2019). These rapid, high-amplitude fluctuations of cumulus clouds have a significant impact on power generation efficiency at both spatial and temporal scales (Perez et al. 2016).

New York State (NYS) features a unique complex terrain, spanning a mix of mountains, lakes, rivers, coastal areas, and major urban centers. Air flows over NYS are modified by synoptic-scale advection process, gravity waves, and land–atmosphere interactions. The mountains and valleys produce mesoscale organized motions such as mountain–valley circulation. The surface wind would also be affected by orographically induced microscale turbulent mixing. Additionally, the heterogeneous land use consisting of lakes, coastal areas, and the mosaic of forest and farmland further complicate the land surface and atmosphere exchange processes, challenging the model to capture the transition from one to the other. All these characteristics provide a good testbed for understanding the impact of complex terrain on BLCs development.

Through interaction with the large-scale flow, the land surface coupled with planetary boundary layer (PBL) and radiation influences the surface energy balance, vertical motion within the boundary layer, and entrainment at the top. These physical processes are essential to cloud formation and morphology, through the partitioning and transporting of moisture and heat in the boundary layer. Consequently, the combination of land surface models (LSMs) and PBL schemes in the model is of critical importance in understanding the coupling of land surface and atmosphere and in simulation of boundary clouds (Bhowmick and Parker 2018; Skamarock et al. 2008). Furthermore, the parameterization of unresolved or subgrid-scale (SGS) clouds and their connection to SGS turbulence in a PBL scheme is critical to improve the simulation of boundary layer cumulus cloud development and surface radiation budget (Angevine et al. 2018; Olson et al. 2019). Previous studies show that surface fluxes simulated by different LSMs would result in changes in the cloud initiation, convection strength, and precipitation intensity of boundary layer clouds (Cutrim et al. 1995; Pielke et al. 1997; Trier et al. 2004; Taylor and Ellis 2006; Taylor et al. 2007; Wang et al. 2009; Garcia-Carreras et al. 2010; Guillod et al. 2014;

Corresponding author: Qilong Min, qmin@albany.com

DOI: 10.1175/WAF-D-21-0172.1

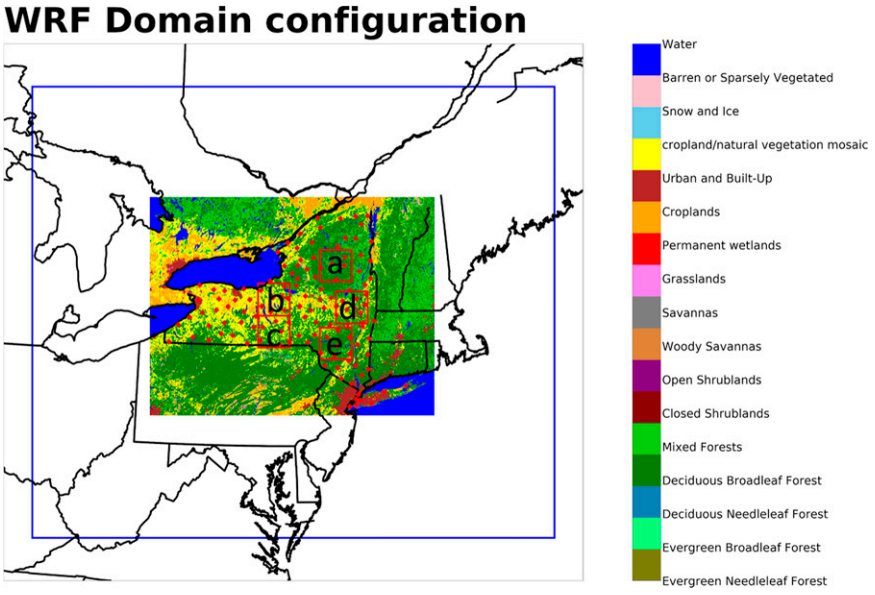

FIG. 1. The vegetation type of the model 1-km domain. The blue box indicates the outer 3-km domain. The red boxes indicate the five regions of interest in this research (labeled with lowercase letters): a is Adirondack, b is Central Lakes, c is Eastern Plateau, d is Hudson Valley, and e is Catskill.

Min et al. 2021). The impacts of different PBL schemes have been studied on heavy rainfall (Efstathiou et al. 2013; Schwitalla et al. 2020; Lv et al. 2020; Potvin et al. 2020), marine stratocumulus clouds (Lamraoui et al. 2019), and convective boundary layer features (Milovac et al. 2016). However, research about coupling impact of LSMs and PBL schemes on boundary layer clouds development over complex terrain is limited.

Over complex terrain, model resolutions strongly affect the model simulation. The higher resolution, the better the model represents land surface heterogeneity. Previous studies show that with more accurate terrain representation in higher resolutions, the model can improve simulations of surface 10-m winds (Serafin and Zardi 2010; Schmidli et al. 2018), generate better spatial distribution and temporal evolution of boundary layer clouds (Langhans et al. 2012; Barthlott and Hoose 2015). The higher model resolution also improves the formation of rainbands and embedded convection (Cosma et al. 2002; Fuhrer and Schär 2007; Kirshbaum 2011).

The motivation of this paper is to gain understanding of land surface–atmosphere–cloud interactions, focusing on the model sensitivity of surface meteorology and boundary layer clouds in terms of various LSMs and PBL schemes, as well as model resolution, over the complex terrain of NYS.

2. Data and method

a. *Model configuration and regions of interest*

This sensitivity study uses WRF-ARW version 4.1 (Skamarock et al. 2019) driven by the High-Resolution Rapid Refresh, version 3 (HRRRv3; Benjamin et al. 2016). The model is configured with two domains: the outer domain with relative coarse grid spacing of 3 km (440 × 380 grid cells) and the inner domain with relatively fine grid spacing of 1 km (718 × 550 grid cells) with 60 vertical layers. As shown in Fig. 1, the outer domain covers a large part of the Northeast United States (NEUS), which is selected based on the correlation analysis of seasonal atmospheric circulation and precipitation to capture the impact of large-scale circulation on the local weather within NYS. The inner domain covers the New York State. For all low-resolution simulations, a single domain with 3-km horizontal resolution (440 × 380 grid cells) is used. The parameterizations and schemes are chosen to be consistent with HRRRv3 in the control run. Thompson aerosol-aware parameterization (Thompson and Eidhammer 2014) is used as microphysics scheme and the Rapid Radiative Transfer Model for GCMs (RRTM-G) is used to estimate radiative forcing (Iacono et al. 2008). To better represent direct and indirect effects of aerosols, daily forecasted aerosols from the GEOS-FP forecast (Rienecker et al. 2008; Molod et al. 2012), which is operated by NASA's Global Modeling and Assimilation Office (GMAO), is used for RRTMG to account the direct aerosol radiative forcing and for Thompson microphysics parameterization to account the indirect aerosol effects, respectively.

The climate and land use characteristics of New York State provides us a great opportunity to investigate the land surface atmosphere interaction over complex terrain. To better evaluate the model performance on warm season convective clouds, five representative regions are selected, shown in Fig. 1, including the following:

- Adirondack—featuring mountains and deciduous forests,
- Central Lakes—flat with mainly farmland,
- Eastern Plateau—relatively flat with farmland,
- Hudson Valley—the intersection of Hudson and Mohawk Valley with farmland and urban surface,
- Catskill—featuring mountains and deciduous forests.

TABLE 1. Summary of WRF v4.1 experiment set.

	Horizontal resolution	Vertical resolution	Subgrid cloud	LSM	PBL	Surface layer
HRRRv3	3 km	50 levels	On	RUC	MYNN-EDMF (hybrid)	MYNN
3km_50levels	3 km	50 levels	On	RUC	MYNN-EDMF (hybrid)	MYNN
1km_60levels	1 km	60 levels	On	RUC	MYNN-EDMF (hybrid)	MYNN
3km_50levels_sgs0	3 km	50 levels	Off	RUC	MYNN-EDMF (hybrid)	MYNN
1km_60levels_sgs0	1 km	60 levels	Off	RUC	MYNN-EDMF (hybrid)	MYNN
RUC_MYNN	1 km	60 levels	On	RUC	MYNN-EDMF (hybrid)	MYNN
RUC_ACM2	1 km	60 levels	None	RUC	ACM2 (hybrid)	Pleim–Xiu scheme
RUC_SH	1 km	60 levels	Off	RUC	SH scale aware (nonlocal)	Revised MM5 scheme
NoahMP_MYNN	1 km	60 levels	On	NoahMP	MYNN-EDMF (hybrid)	MYNN
NoahMP_ACM2	1 km	60 levels	None	NoahMP	ACM2 (hybrid)	Pleim–Xiu scheme
NoahMP_SH	1 km	60 levels	None	NoahMP	SH scale aware (nonlocal)	Revised MM5 scheme

b. *Experimental design*

In this experiment, the WRF Model performs 24-h simulations, started daily at 0000 UTC, in reforecast mode. Nine sensitivity simulations are conducted to investigate three factors that potentially affect the simulation of boundary layer clouds: 1) the model resolution, 2) the model physical parameterizations of land surface and boundary layer, and 3) the model parameterization of SGS cloud processes. The specific settings of the sensitivity experiments are summarized in Table 1. It is worth noting that the experiment RUC_MYNN is the same as 1km_60levels.

On the model resolution, we choose the horizontal grid spacing of 3 km and the vertical resolution of 50 levels as the control run to be consistent with the HRRRv3 model configuration. To better represent the complex terrain over NYS, we also increase the horizontal grid spacing to 1 km and correspondingly increase the vertical resolution to 60 levels. For the extra 10 vertical layers, 6 layers were added in the PBL and the other 4 layers were in the rest of atmosphere. It is anticipated that the simulations with higher resolution would better simulate the boundary layer processes, such as capping inversion, sharp wind shear, low-level jets, and boundary layer clouds. As the SGS processes have implication of model resolutions, we further conduct the sensitivity studies by turning off the SGS cloud coupling to radiation scheme by setting the namelist parameter icloud_bl = 0 in the Mellor–Yamada–Nakanishi–Niino eddy diffusivity mass flux (MYNN-EDMF) PBL scheme for both low-resolution (3 km × 50 level) and high-resolution (1 km × 60 level) simulations.

On model physics and SGS process, we conduct six sensitivity simulations with combinations of two land surface models (LSMs) and three PBL schemes. The different combination of LSM and PBL parameterizations would provide different representation of surface–atmosphere exchange processes. In addition to the Rapid Update Cycle (RUC) that is used in HRRRv3 (Smirnova et al. 2016), we also test the widely used NoahMP LSM (Niu et al. 2011; Yang et al. 2011). These two models vary in soil hydrological processes, surface exchange coefficients and the formulation of heat and moisture fluxes. The RUC LSM includes nine soil levels, uses the Richards equation to solve for heat transfer, and includes gravitational impacts on soil moisture. A special feature of RUC LSM is a thin layer spanning the ground surface that includes half of the first atmospheric layer and half of the top soil layer to solve the energy budgets and surface energy balance. RUC LSM uses the surface exchange coefficients from the surface-layer schemes. The latent heat flux is directly affected by vegetation through incorporation of evapotranspiration and intercepted water from canopy. NoahMP LSM is an extended version of Noah, with an internal suite of physical parameterizations and a modified energy balance equation and solves for its own exchange coefficient (Niu et al. 2011; Yang et al. 2011). NoahMP predicts soil moisture and temperature in four layers with layer thickness of 10, 30, 60 and 100 cm, respectively, from top to bottom. NoahMP calculates canopy energy balance separated from surface energy balance, better representing vegetation interaction with the atmosphere. The runoff parameterization depends on soil types and accounts for the role of heterogeneities in soil moisture and terrain, potentially improving the soil hydrological processes over complex terrain (Ma et al. 2017).

We select three PBL schemes using hybrid and nonlocal assumptions to understand their impact on boundary layer cloud development. Specifically, we test MYNN-EDMF (Olson et al. 2019)—a turbulent kinetic energy (TKE)-based PBL scheme, which is improved from the MYJ (Janjić 2001) and MYNN PBL schemes (Mellor and Yamada 1982; Nakanishi and Niino 2004, 2009). In this study, we turn on the mass-flux component (set bl_mynn_edmf = 1) in MYNN-EDMF to enable the representation of nonlocal mixing using an eddy-diffusivity approach tied to TKE. One of the main features of MYNN-EDMF scheme is to use cloud probability distribution functions (PDFs) to represent SGS clouds and associated SGS turbulence. In the cloud PDFs, the resolved-scale fields are used to determine the SGS cloud mixing ratio, cloud fraction, and the buoyancy flux. Those SGS macrophysical properties are used to parameterize the SGS buoyancy flux and further coupled into other WRF physics schemes (e.g., radiation scheme). A nonlocal Shin–Hong (SH) scale-aware scheme (Shin and Hong 2015) that based on the Yonsei University PBL (YSU) scheme (Hong et al. 2006) is also tested. In this scheme, the nonlocal transport by large eddies and local

transport by small-scale eddies are calculated separately. The SGS turbulence is formulated by multiplying a grid-size dependency function with the total nonlocal transport profile fitted to the LES output. We also test the Asymmetric Convective Model 2 (ACM2) (Pleim 2007a,b), which uses a combination of local (a first-order eddy diffusion scheme) and nonlocal transport that switches off smoothly to local eddy diffusion in stable environments. For very stable conditions, the slope of the stability functions in ACM2 is reduced to permit significant fluxes to occur, which could particularly improve nocturnal surface forecasting.

c. *The postfrontal event*

During warm season over NEUS, the land surface airmass modification during postfrontal events is an important process that impacts mixed layer thermodynamic profiles. The buildup of heat and humidity during this period is essential for the development of boundary layer cumulus clouds. Specifically, we select a postfrontal event from 24 to 27 July 2019 to investigate the sensitivity of surface thermodynamic conditions to different model configurations. On 22 July 2019, severe thunderstorms occurred over almost the whole New York State. Rain continued through 23 July 2019 until the passage of a cold front brought fresh cold and dry air to our research domain. From 24 to 27 July 2019, there was a sequence of undisturbed fair-weather days featuring boundary layer cumulus clouds and some isolated showers in the afternoon. During this postfrontal event, local surface atmosphere exchange modified the air mass, and heat and moisture continued to build up. Surface moisture fluxes from forests and grassland moistened the atmosphere through evapotranspiration and further facilitated the formation of boundary layer cumulus clouds (Freedman et al. 2001; Freedman and Fitzjarrald 2001).

d. *Data*

1) New York State Mesonet

University at Albany and the NYS Division of Homeland Security and Emergency Services established the NYS Mesonet in 2014. NYS Mesonet is a dense meteorological network of 126 standard weather stations providing data of surface temperature, humidity, wind speed and direction, solar radiation, atmospheric pressure, snow depth, and soil temperature and moisture at every 5 min. Additionally, NYS Mesonet has a sophisticated profiling network of 17 enhanced sites and 17 flux sites for latent heat and sensible heat fluxes and other measurements. These high-resolution datasets provide comprehensive measurements of the meteorology, land surface conditions, and land surface–atmosphere interaction.

2) GOES satellite cloud optical depth

The Geostationary Operational Environmental Satellite GOES-R Series is NOAA's latest generation of geostationary weather satellites. The Advanced Baseline Imager (ABI) is the primary imaging instrument on *GOES-16* with 16 spectral bands at high spatiotemporal resolutions (Hillger and Schmit 2004; Clarke 2010). *GOES-16*-retrieved products of cloud properties are used in this study, including cloud and moisture imagery, and cloud optical depth.

3. Results

a. *Impacts of model resolution*

The complex terrain produces organized motion at multiscales, influencing cloud development and local meteorology, particularly during postfrontal events. Model representations of such terrain induced motions and other associated physical processes are sensitive to resolution, both horizontal and vertical. Figures 2 and 3 illustrate differences of WRF forecasting between the control resolution of 3 km × 50 levels and the enhanced resolution of 1 km × 60 levels at two NYSM sites, Claryville (CLAR) and Voorheesville (VOOR), respectively. The NYSM Claryville site is located in a valley in the Catskill Mountains, where the 1-km resolution terrain shows the contrast between valley and ridges while 3-km resolution terrain is relatively flat. The NYSM Voorheesville site is located at the cross of Hudson Valley and Mohawk Valley, and at the southern side of Helderberg Mountain (Helderberg Escarpment). The sharp elevation increase in the south is well represented in the 1-km resolution but is relatively smoothed in the 3-km resolution. For both sites, the comparison of WRF forecasts of different resolutions at both sites consistently show that the 1-km high-resolution simulation predicts more turbulence fluctuation in surface wind speed at 10 m, which is closer to the NYSM observation. For CLAR site, the mean bias of high-resolution run is 0.66 m s^{-1} compared to 1.24 m s^{-1} for the low-resolution run. Specifically, the nocturnal wind speed is noticeably improved (the mean nocturnal bias of high-resolution run is 0.79 m s^{-1} compared to 1.93 m s^{-1} for low-resolution run), showing a stronger diurnal cycle and the improvement by using 1-km resolution is noticeable at night. In the meantime, for both observation and model simulations, the VOOR site does not show clear diurnal variations as CLAR. It is possible that due to better representing complex topography, the nighttime 2-m temperatures are better captured by high-resolution simulation at the CLAR site on 24 and 25 July 2019. During the daytime, the value of mean bias of specific humidity and temperature at both sites is smaller in the low-resolution simulations. Furthermore, both sites show that the simulations of 3 km × 50 level resolution have much smoother surface meteorology, which are consistent with HRRRv3 forecasting. For both sites, the observed shortwave radiation shows rapid fluctuations caused by passage of locally formed cumulus clouds. The 1-km resolution WRF forecasting in solar radiation is consistent with NYSM observation, exhibiting variability of cloud fields. It suggests that the temporal variability of cumulus clouds is better simulated in the high-resolution simulation than in the low-resolution simulation.

b. *Impacts of model physics configuration*

Land–atmosphere interactions consistent a multitude of processes that link the land surface to the atmospheric boundary layer, with feedbacks of coupled processes. Model utilizes LSMs and PBL schemes and their interactions to represent

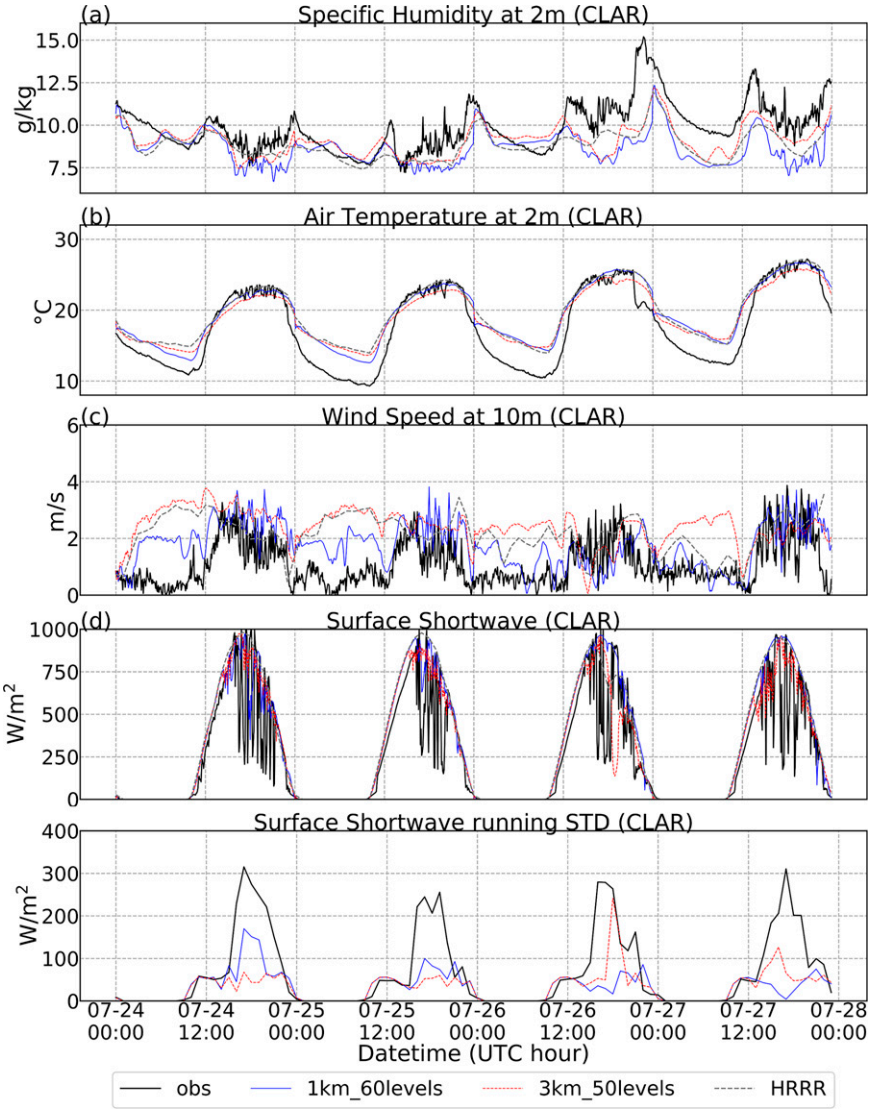

FIG. 2. The 5-min resolution time series of (a) 2-m specific humidity, (b) 2-m air temperature, (c) 10-m wind speed, (d) surface downward solar radiation, and (e) solar radiation standard deviation from 1-h running mean of different model resolution simulation and observation at the NYSM Claryville (CLAR) site.

the exchanges of energy and water vapor between land and atmosphere. As discussed in section 2b, we conduct six sensitivity simulations with combinations of two LSM models, RUC and NoahMP, and three PBL schemes, MYNN-EDMF, ACM2, and SH scale aware. As shown in Fig. 4, the averaged surface meteorology over 126 NYSM sites is controlled primarily by the land surface models. Both RUC and NoahMP are initialized with the HRRRv3 grids, which have nine soil layers as in RUC, while NoahMP have four soil layers. It is anticipated that sensitivity runs with RUC model are consistent with HRRRv3, as the soil state is more consistently with initial condition in RUC compared to NoahMP. This may be the fundamental reason why the RUC performs better than NoahMP in this study. The result shows sensitivity runs with NoahMP runs exhibit the dry and warm biases compared to RUC runs in daytime. At nighttime, NoahMP runs simulate drier and colder atmosphere, leading to overall improvement of simulations. The daytime dry and warm biases generally increase as the postfrontal event progresses, even though all simulations are started at 0000 UTC every day. Although NoahMP based simulations show a larger warm and dry bias compared to that of RUC, they predict smaller solar radiation bias at most NYSM sites.

The impacts of PBL schemes on simulated surface meteorology are relatively smaller to that of LSMs. It is interesting that the ACM2 scheme coupled with NoahMP produces consistently lower values of temperature, specific humidity, and wind speed at most NYSM sites, while the SH scale-aware

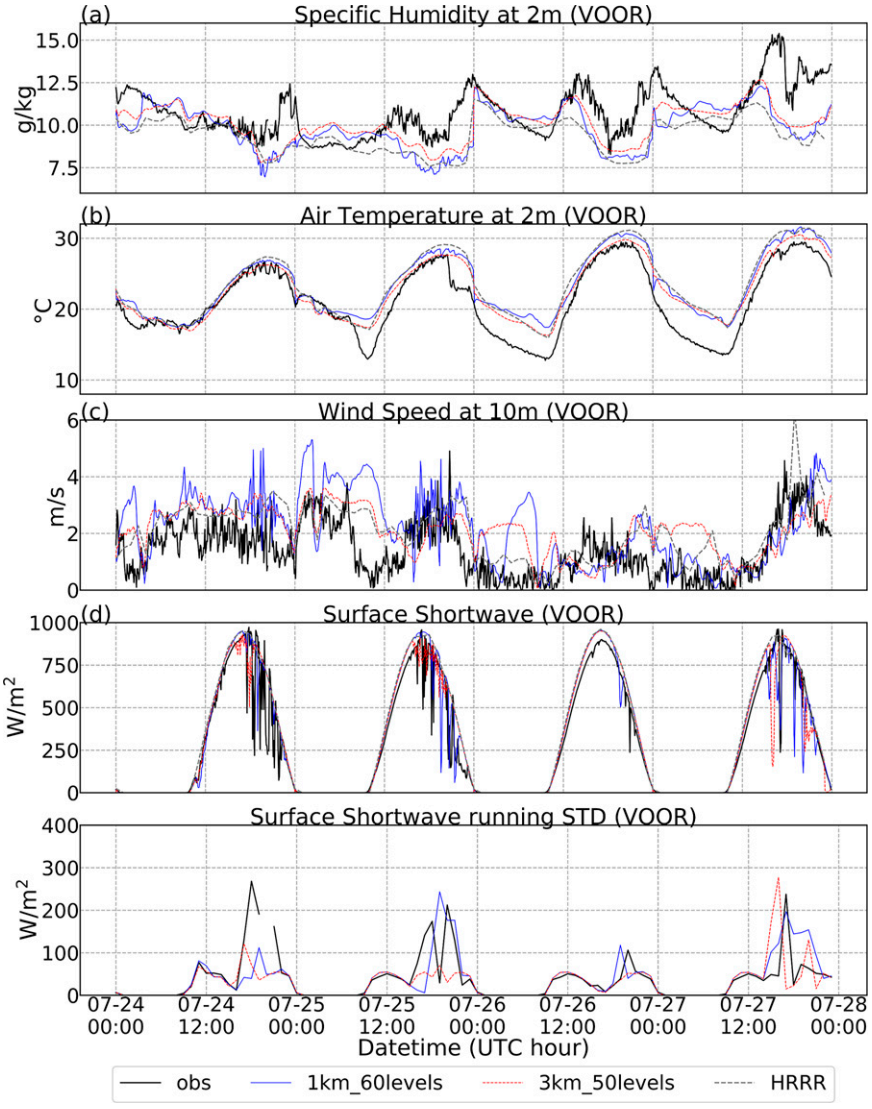

FIG. 3. As in Fig. 2, but for the NYSM Voorheesville (VOOR) site.

scheme coupled with RUC produces lower values of surface meteorology at most sites. The MYNN-EDMF scheme, coupled with either RUC or NoahMP, predicts the middle values of surface meteorology among all three PBL schemes.

To gain a better understanding of the impact of land surface models on surface meteorology, the surface energy partitions are investigated at two NYSM sites, where surface flux measurements are available, one over forest (NYSM Redfield site) and another over farmland (NYSM Ontario site). Figure 5 shows that the RUC-MYNN combination tends to predict higher evaporative fraction than that of NoahMP-MYNN over both farmland and forest sites. The difference in evaporative fraction between these two LSMs is due to different parameterizations of vegetation impacts on evapotranspiration process. RUC uses plant coefficients determined by vegetation type to represent resistance, while NoahMP parameterizes canopy resistance in terms of four environmental stress function (Jarvis 1976; Ball et al. 1987). Additionally, RUC calculates soil temperature and moisture at nine soil layers with a depth of 3 m, while NoahMP considers four soil layers from 0 to 2 m. These differences in soil hydrological process representation and evapotranspiration parameterization would directly affect the partition of surface energy and predict different surface heat fluxes. Consequently, the higher latent heat fluxes in RUC-MYNN simulation may transfer more moisture into the atmosphere, resulting in relatively greater specific humidity at 2 m (not shown here) than that in NoahMP-MYNN simulation. In the meantime, the lower sensible heat fluxes in RUC-MYNN simulation may result in a cooler air temperature at 2 m than that in NoahMP-MYNN simulation.

As illustrated in Fig. 5 and discussed above, the forecasted surface meteorology is sensitive to the Bowen ratio (BR) or evaporative fraction (EF) predicted by land surface models. Figure 6 shows the comparison of Bowen ratio predicted by

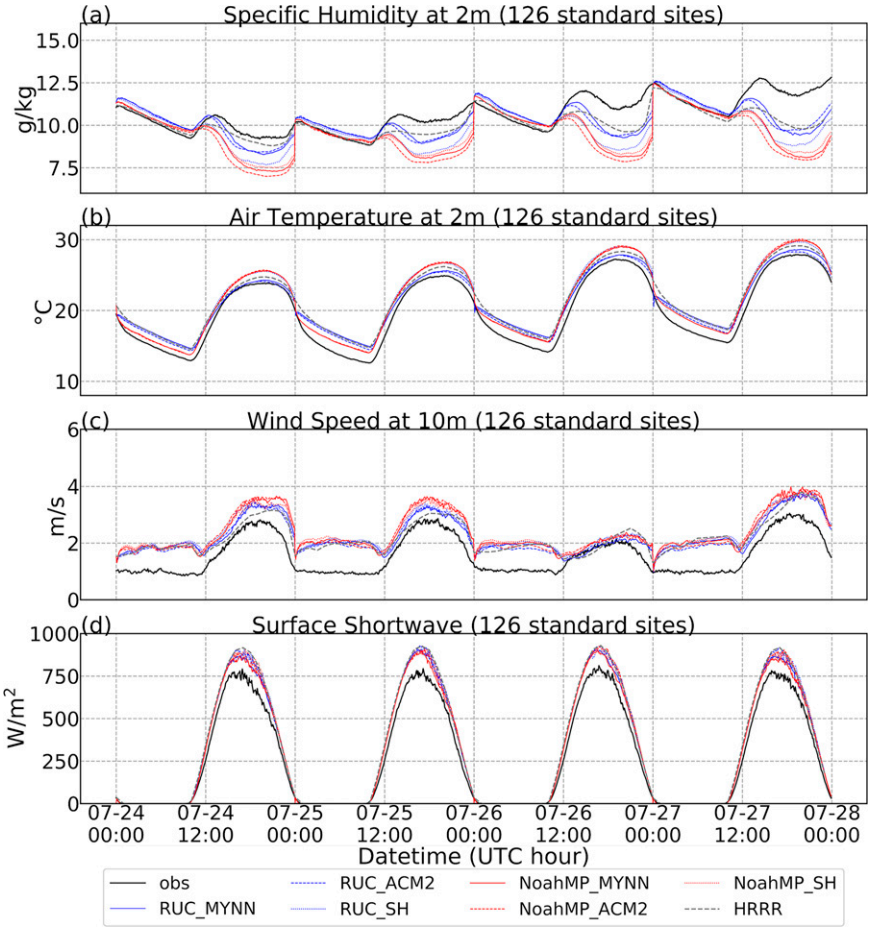

FIG. 4. The 5-min resolution time series of 126 sites averaged (a) 2-m specific humidity, (b) 2-m air temperature, (c) 10-m wind speed, and (d) surface downward solar radiation of different model physics simulations and observation.

both RUC-MYNN and NoahMP-MYNN combinations over the simulation domain, containing entire NYS. The RUC-MYNN simulation predicts much lower Bowen ratio than that of the NoahMP-MYNN simulation. The spatial pattern of the Bowen ratio is consistent with land-use types with large contrast between farmland and forest, i.e., Bowen ratios over forest dominated regions (noticeable in Adirondack and Catskill regions) are significantly lower than the farmland dominated regions. The contrast surface energy partition of latent heat and sensible heat represented by predicted Bowen ratio in the RUC and NoahMP LSMs largely explains the difference of forecasted surface meteorology by these two models.

Boundary layer cumulus cloud formation is impacted by thermodynamic processes in the boundary layer, as a result of land–atmosphere interaction. The sensitivity study with different combinations of two LSMs and three PBL schemes enable us to better understand those impacts on cumulus clouds. Figure 7 displays cloud optical depth snapshots at 1800 UTC 24 July 2019 of six combinations of LSM-PBL. The simulations using NoahMP scheme produce more clouds than the RUC based simulations, and consequently less solar radiation bias as compared with NYSM observation (Fig. 4d) (the NYSM observation mean solar radiation bias of RUC based simulation is 78.84 W m^{-2} and NoahMP based simulation biases is 73.99 W m^{-2}). As discussed above, the Bowen ratio is higher in NoahMP based simulations. The higher Bowen ratio indicates stronger sensible heat that may enhance the strength of vertical mixing, deepen boundary layer (see Fig. 8) and may further promote the development of boundary layer clouds, but also indicates lower latent heat that may reduce the moisture supply from the surface to the atmosphere therefore suppress the development of boundary layer clouds.

The PBL schemes affect cloud formation, evident in the simulated cloud optical depth, shown in Fig. 7. Coupled with either RUC or NoahMP LSMs, the MYNN-EDMF scheme with the SGS clouds (more discussion below) produce the most cloud coverage, closer to the GOES observation (Fig. 10a). The ACM2 scheme predicts more clouds than that of the SH scale-aware schemes. At the grid spacing of 1 km, clouds and boundary layer turbulence can be partially resolved in the model. Therefore, the boundary layer clouds should be affected by the strength and distribution of resolved updrafts in the middle of

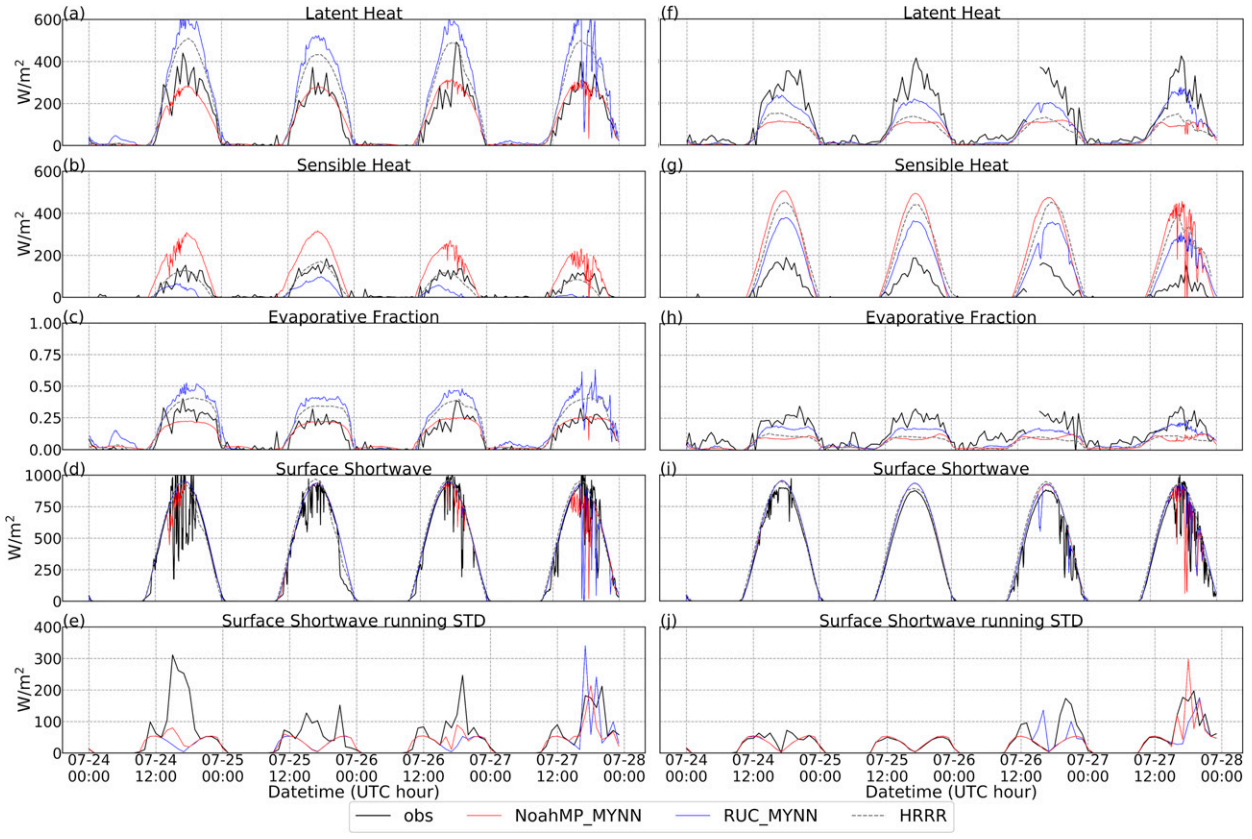

FIG. 5. The 5-min resolution time series of (a) latent heat, (b) sensible heat, (c) evaporative fraction, (d) surface downward solar radiation, and (e) solar radiation standard deviation from the 1-h running mean of different land surface model simulations and observation at (left) the NYSM Redfield (REDF) forest site and (right) the NYSM Ontario (ONTA) farmland site.

PBL. Figure 9 shows that the SH scale-aware PBL scheme resolves more updrafts and produced strongest convective strength in the PBL, and ACM2 PBL scheme rarely resolve convection even at 1-km resolution. The strength of convection and resolved updraft produced by MYNN-EDMF is in the middle. Therefore, although the SH scale-aware scheme predicts the smallest cloud coverage in the domain, for individual cumulus clouds in a narrow region, the SH scale-aware scheme predicts the largest cloud optical depth, while the ACM2 scheme products the smallest cloud optical depth with the weakest convection.

c. *Impacts of subgrid cloud*

Among the three tested PBL schemes, the MYNN-EDMF scheme predicts the lowest bias in surface downward solar radiation (Fig. 4d). As discussed in section 2b, the MYNN-EDMF

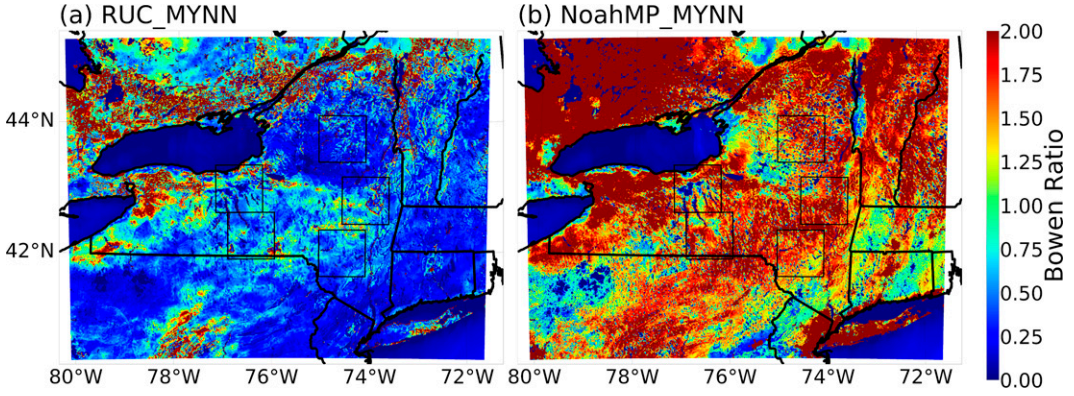

FIG. 6. Model-simulated Bowen ratio for two different land surface models: (a) RUC and (b) NoahMP over the domain of New York State at 1800 UTC (1300 LT).

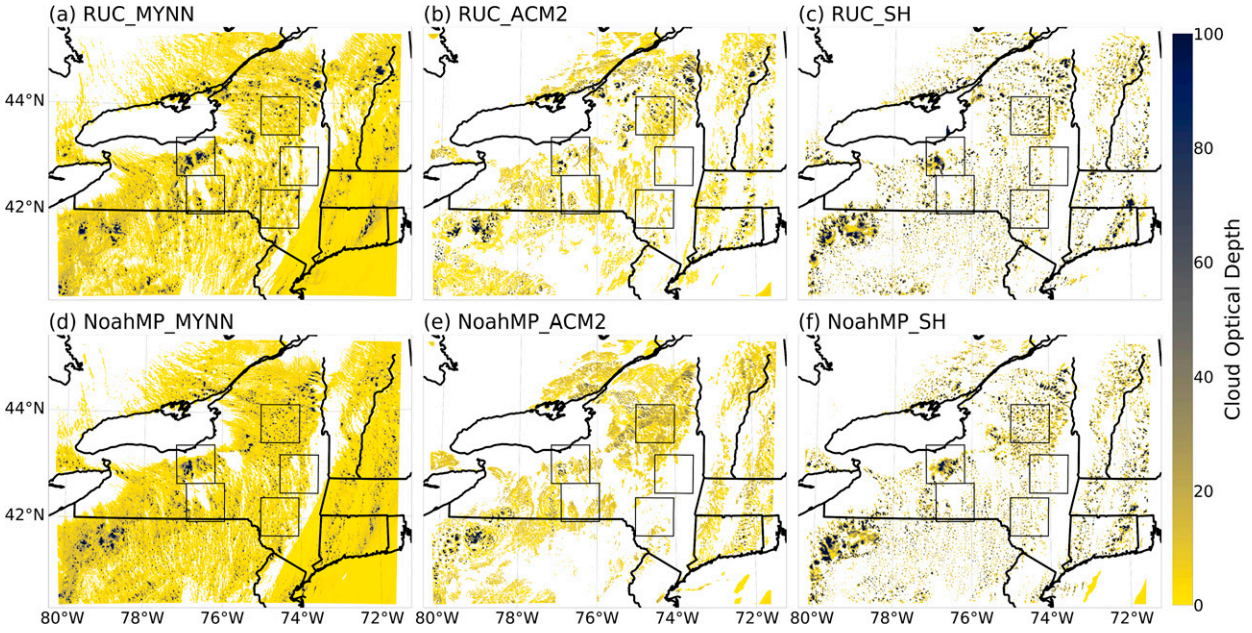

FIG. 7. Snapshot of simulated cloud optical depth at 1800 UTC 24 Jul 2019 for different model physics. (top) The RUC land surface model with (a) MYNN-EDMF PBL scheme, (b) ACM2 hybrid PBL scheme, and (c) SH scale-aware nonlocal scheme. (bottom) The NoahMP land surface model with (d) MYNN-EDMF PBL scheme, (e) ACM2 hybrid PBL scheme, and (f) SH scale-aware scheme.

scheme blends a non-convective subgrid component with a mass-flux component (Chaboureau and Bechtold 2002, 2005). It determines the SGS cloud mixing ratio, cloud fraction, and the buoyancy flux using the higher-order moments or vertical gradients of the resolved-scale fields, i.e., producing clouds when relative humidity and the variance of the saturation deficit are sufficiently large. In the current MYNN-EDMF scheme, the SGS clouds are only coupled into the WRF radiation schemes, when the namelist parameter icloud_bl is set to 1.

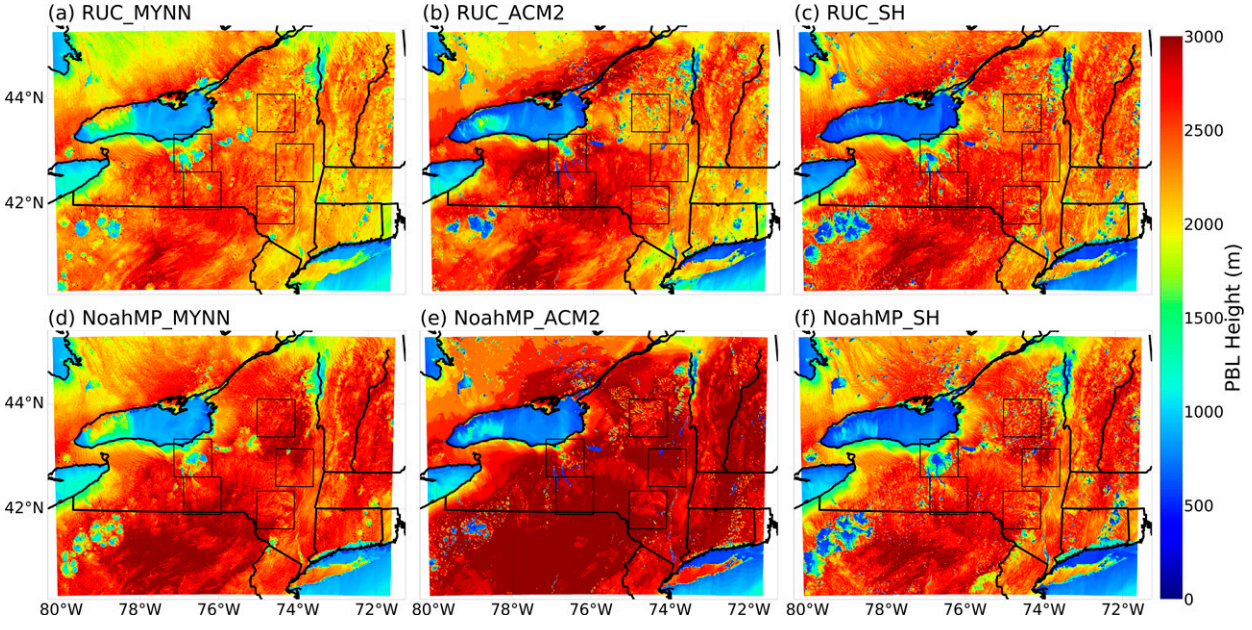

FIG. 8. Model-simulated horizontal distribution of boundary layer height for different model physics over the domain of New York State at 1800 UTC (1300 LT). (top) The RUC land surface model with (a) MYNN-EDMF PBL scheme, (b) ACM2 hybrid PBL scheme, and (c) SH scale-aware nonlocal scheme. (bottom) The NoahMP land surface model with (d) MYNN-EDMF PBL scheme, (e) ACM2 hybrid PBL scheme, and (f) SH scale-aware scheme.

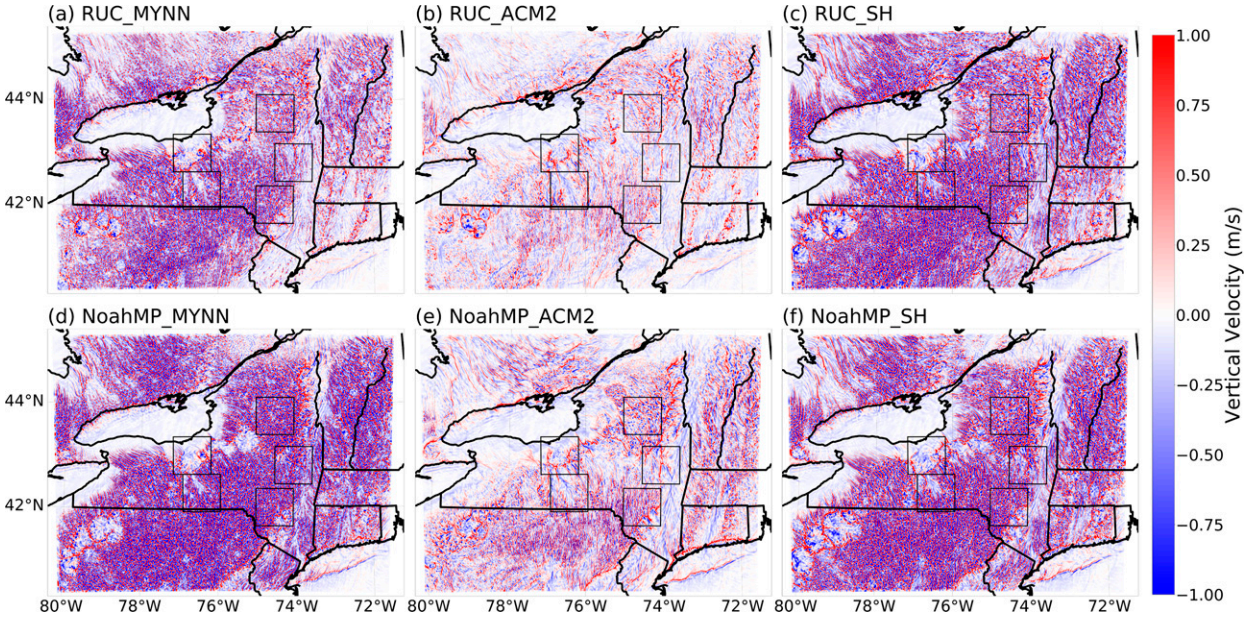

FIG. 9. Model-simulated horizontal distribution of vertical velocity at 850 hPa for different model physics over the domain of New York State at 1800 UTC (1300 LT). (top) The RUC land surface model with (a) MYNN-EDMF PBL scheme, (b) ACM2 hybrid PBL scheme, and (c) SH scale-aware nonlocal scheme. (bottom) The NoahMP land surface model with (d) MYNN-EDMF PBL scheme, (e) ACM2 hybrid PBL scheme, and (f) SH scale-aware scheme.

Figure 10 shows the comparison of *GOES-16* observed clouds with outputs of two sets of WRF sensitivity simulations: 1) on or off of the SGS clouds and its coupling of SGS clouds into the WRF radiation scheme; and 2) model resolution of 1 km × 60 level versus 3 km × 50 level. The total cloud optical depth in Figs. 10b and 10d adds SGS cloud optical depth calculated from MYNN-EDMF scheme as SGS clouds are turned on, whereas in Figs. 10c and 10e the SGS clouds are

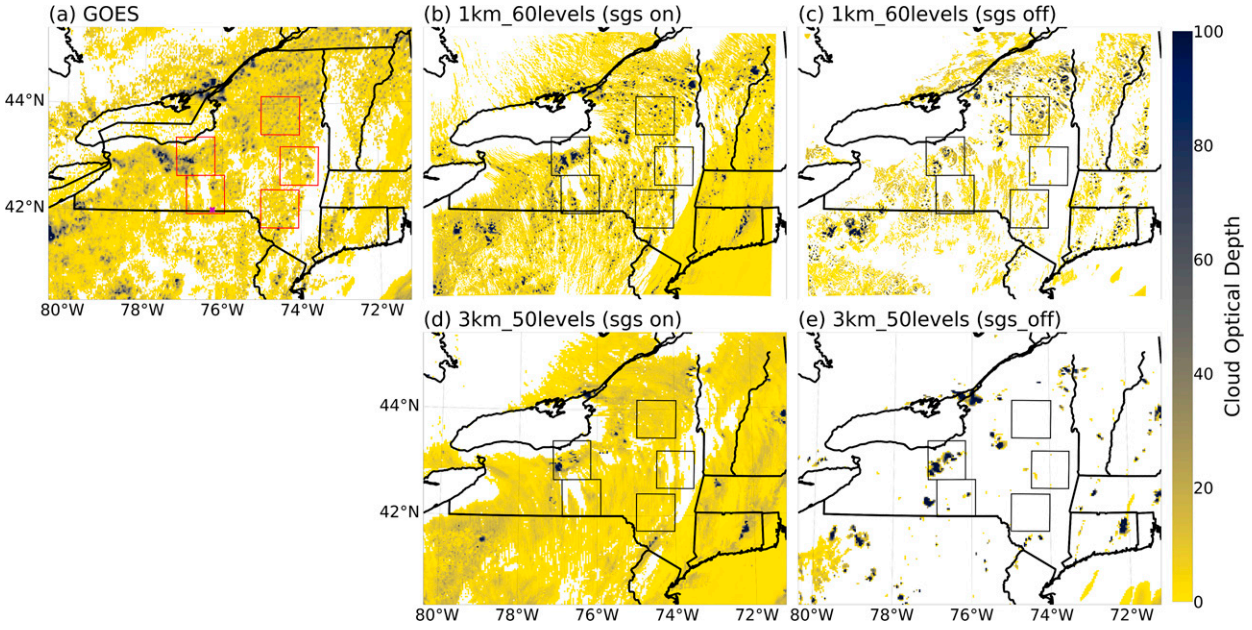

FIG. 10. Snapshot of observed and simulated cloud optical depth at 1800 UTC 24 Jul 2019. (a) GOES observed cloud optical depth, (b) cloud optical depth with SGS turn on for high-resolution (1km_60levels) simulation, (c) cloud optical depth with SGS turn off for high-resolution (1km_60levels_sgs0), (d) cloud optical depth with SGS turn on for low-resolution (3km_50levels) simulation, and (e) cloud optical depth with SGS turn off for low-resolution (3km_50levels_sgs0) simulation.

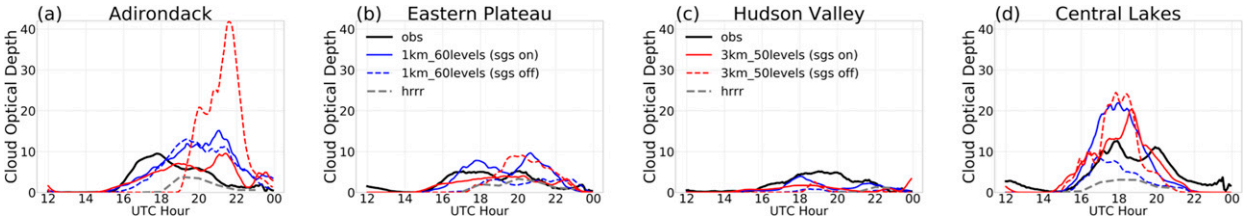

FIG. 11. Time series of domain-averaged cloud optical depth over four selected regions from 1200 to 2400 UTC (0700–1900 LT) 24 Jul 2019.

turn off. The MYNN-EDMF with SGS on predicts the cloud fields that are consistent with GOES satellite observation (Fig. 10a). The optical depth is greatly reduced with the SGS clouds uncoupled to the radiation for both model resolution simulations (icloud_bl = 0). As discussed in the section on the model resolution, the high-resolution simulation generally produces more clouds than the low-resolution simulation does. Even when the SGS clouds are turned off, the high-resolution simulation predicts scattered cumulus clouds, much better than the low-resolution simulation.

To better understand the impacts of the coupling of the MYNN-EDMF SGS cloud with radiation, the time series of domain averaged cloud optical depth are compared in Fig. 11, for the four regions discussed in section 2c. The time series suggest that the SGS cloud scheme is more important for the low-resolution simulation (3 km × 50 level), where the cumulus clouds are hardly resolved. Over the Adirondack region, where the boundary layer clouds occur most frequently, for the low-resolution simulations, the convective component of boundary layer clouds only initiates after 1900 UTC (the red dash line), while the non-convection component initiate around 1500 UTC, which is consistent with the observation. For the high-resolution simulations, some cumulus clouds are already resolved even with the SGS turn-off, and the MYNN-EDMF with SGS on further improves the prediction of clouds and consequently solar radiation.

4. Conclusions

Prediction of regional weather and climate for a region such as the New York State with its complex terrain and land use constitutes a major challenge. One of the major limitations to our ability to address the challenge is a lack of high-resolution observations that enable accurate understanding and parameterizing detailed scale-dependent processes, linking land surface properties to boundary layer and atmospheric properties. NYSM provides high-resolution measurements of 126 standard weather stations, plus 17 flux sites for latent heat and sensible heat fluxes and other measurements. In this study, we utilize NYSM high-resolution observations to conduct a set of sensitivity studies, accessing impacts of various WRF LSM models and PBL schemes on forecasting accuracy. As both complex topography and land cover can modify moist inflow to clouds, specifically, we focus on three factors that may affect the simulation accuracy of boundary layer clouds: 1) the model resolution (1 km × 60 level versus 3 km × 50 level), 2) the model physical parameterizations (two LSMs—RUC and NoahMP and three BPL schemes—MYNN-EDMF, ACM2, and SH scale aware), and 3) the model parameterization of SGS processes (MYNN-EDMF SGS). In the meantime, we use the state-of-art HRRRv3 forecasting as reference for the sensitivity evaluation.

Given the complex terrain of NYS, the high-resolution simulations (1 km × 60 level) predict better surface meteorology and cloud fields than the low-resolution simulations (3 km × 50 level). The evaluation of sensitivity simulations against NYSM observations suggests that surface meteorology is controlled primarily by the land surface models, and secondarily by the PBL schemes. Among six combinations of two LSMs and three PBL schemes, the RUC-MYNN combination tends to predict higher evaporative fraction or lower Bowen ratio than that of NoahMP-MYNN over NYS. The difference in predicted Bowen ratio by the RUC and NoahMP LSMs may result in the difference of forecasted surface meteorology, where RUC based simulations have lower biases than those of NoahMP based simulation.

The different PBL schemes have different impacts on cloud formation, as evident by simulated cloud optical depths. The MYNN-EDMF scheme with the SGS produces the highest cloud cover, closer to the GOES observation, and thus predicts the lowest bias in surface solar radiation. The temporal evolution of simulated cloud fields suggests that the SGS scheme is more important for the low-resolution simulations (3 km × 50 level) than for the high-resolution simulations. Although some cumulus clouds are already resolved in the high-resolution simulations even with the SGS turn-off, the MYNN-EDMF with SGS further improve the prediction of cloud fields for the high-resolution simulations.

The sensitivity study provides further understanding of land surface–atmosphere processes on weather forecasting and is useful for renewable energy forecasting and management.

Acknowledgments. This work was supported by the U.S. Department of Energy, Energy's Office of Energy Efficiency and Renewable Energy (EERE) under the Solar Energy Technologies Office Award 33504, and by the National Oceanic and Atmospheric Administration (NOAA) Educational Partnership Program with Minority Serving Institutions Cooperative Agreement NA16SEC4810006.

Data availability statement. The data from New York State Mesonet are available at http://www.nysmesonet.org/weather/requestdata. The HRRR model simulations are available at https://www.nco.ncep.noaa.gov/pmb/products/hrrr/.

REFERENCES

Angevine, W. M., J. Olson, J. Kenyon, W. I. Gustafson Jr., S. Endo, K. Suselj, and D. D. Turner, 2018: Shallow cumulus in WRF parameterizations evaluated against LASSO large-eddy simulations. *Mon. Wea. Rev.*, **146**, 4303–4322, https://doi.org/10.1175/MWR-D-18-0115.1.

Ball, J. T., I. E. Woodrow, and J. A. Berry, 1987: A model predicting stomatal conductance and its contribution to the control of photosynthesis under different environmental conditions. Process in Photosynthesis Research, J. Biggins, Ed., Springer, 221–224, https://doi.org/10.1007/978-94-017-0519-6_48.

Barthlott, C., and C. Hoose, 2015: Spatial and temporal variability of clouds and precipitation over Germany: Multiscale simulations across the "gray zone." *Atmos. Chem. Phys.*, **15**, 12 361–12 384, https://doi.org/10.5194/acp-15-12361-2015.

Bélair, S., J. Mailhot, C. Girard, and P. Vaillancourt, 2004: Boundary layer and shallow cumulus clouds in a medium-range forecast of a large-scale weather system. *Mon. Wea. Rev.*, **133**, 1938–1960, https://doi.org/10.1175/MWR2958.1.

Benjamin, S. G., and Coauthors, 2016: A North American hourly assimilation and model forecast cycle: The Rapid Refresh. *Mon. Wea. Rev.*, **144**, 1669–1694, https://doi.org/10.1175/MWR-D-15-0242.1.

Berg, A., K. Findell, B. R. Lintner, P. Gentine, and C. Kerr, 2013: Precipitation sensitivity to surface heat fluxes over North America in reanalysis and model data. *J. Hydrometeor.*, **14**, 722–743, https://doi.org/10.1175/JHM-D-12-0111.1.

Bhowmick, M., and D. J. Parker, 2018: Analytical solution to a thermodynamic model for the sensitivity of afternoon deep convective initiation to the surface Bowen ratio. *Quart. J. Roy. Meteor. Soc.*, **144**, 2216–2229, https://doi.org/10.1002/qj.3340.

Chaboureau, J. P., and P. Bechtold, 2002: A simple cloud parameterization derived from cloud resolving model data: Diagnostic and prognostic applications. *J. Atmos. Sci.*, **59**, 2362–2372, https://doi.org/10.1175/1520-0469(2002)059<2362:ASCPDF>2.0.CO;2.

——, and ——, 2005: Statistical representation of clouds in a regional model and the impact on the diurnal cycle of convection during Tropical Convection, Cirrus and Nitrogen Oxides (TROCCINOX). *J. Geophys. Res.*, **110**, D17103, https://doi.org/10.1029/2004JD005645.

Clarke, J., 2010: GOES-R ABI Level 1B Solar Channel Data Distribution Study: Analysis of alternatives for utilization of radiance and reflectance factor instrument data. NOAA/NESDIS, 63 pp.

Cosma, S., E. Richard, and F. Miniscloux, 2002: The role of small-scale orographic features in the spatial distribution of precipitation. *Quart. J. Roy. Meteor. Soc.*, **128**, 75–92, https://doi.org/10.1256/00359000260498798.

Cutrim, E., D. W. Martin, and R. Rabin, 1995: Enhancement of cumulus clouds over deforested lands in Amazonia. *Bull. Amer. Meteor. Soc.*, **76**, 1801–1805, https://doi.org/10.1175/1520-0477(1995)076<1801:EOCCOD>2.0.CO;2.

Efstathiou, G., N. Zoumakis, D. Melas, C. Lolis, and P. Kassomenos, 2013: Sensitivity of WRF to boundary layer parameterizations in simulating a heavy rainfall event using different microphysical schemes: Effect on large-scale processes. *Atmos. Res.*, **132–133**, 125–143, https://doi.org/10.1016/j.atmosres.2013.05.004.

Freedman, J. M., and D. R. Fitzjarrald, 2001: Postfrontal airmass modification. *J. Hydrometeor.*, **2**, 419–437, https://doi.org/10.1175/1525-7541(2001)002<0419:PAM>2.0.CO;2.

——, ——, K. E. Moore, and R. K. Sakai, 2001: Boundary layer clouds and vegetation–atmosphere feedbacks. *J. Climate*, **14**, 180–197, https://doi.org/10.1175/1520-0442(2001)013<0180:BLCAVA>2.0.CO;2.

Fuhrer, O., and C. Schär, 2007: Dynamics of orographically triggered banded convection in sheared moist orographic flows. *J. Atmos. Sci.*, **64**, 3542–3561, https://doi.org/10.1175/JAS4024.1.

Garcia-Carreras, L., D. J. Parker, C. M. Taylor, C. E. Reeves, and J. G. Murphy, 2010: Impact of mesoscale vegetation heterogeneities on the dynamical and thermodynamic properties of the planetary boundary layer. *J. Geophys. Res.*, **115**, D03102, https://doi.org/10.1029/2009JD012811.

Guillod, B. P., and Coauthors, 2014: Land-surface controls on afternoon precipitation diagnosed from observational data: Uncertainties and confounding factors. *Atmos. Chem. Phys.*, **14**, 8343–8367, https://doi.org/10.5194/acp-14-8343-2014.

Hillger, D. W., and T. Schmit, 2004: Quantization noise for GOES-R ABI bands. *Proc. 13th Conf. on Satellite Meteorology and Oceanography*, Norfolk, VA, Amer. Meteor. Soc., P1.7, https://ams.confex.com/ams/13SATMET/webprogram/Paper78984.html.

Hong, S. Y., Y. Noh, and J. Dudhia, 2006: A new vertical diffusion package with an explicit treatment of entrainment processes. *Mon. Wea. Rev.*, **134**, 2318–2341, https://doi.org/10.1175/MWR3199.1.

Iacono, M. J., J. S. Delamere, E. J. Mlawer, M. W. Shephard, S. A. Clough, and W. D. Collins, 2008: Radiative forcing by long-lived greenhouse gases: Calculations with the AER radiative transfer models. *J. Geophys. Res.*, **113**, D13103, https://doi.org/10.1029/2008JD009944.

Janjić, Z., 2001: Nonsingular implementation of the Mellor-Yamada level 2.5 scheme in the NCEP Meso Model. NCEP Office Note 437, 61 pp.

Jarvis, P. G., 1976: The interpretation of the variations in leaf water potential and stomatal conductance found in canopies in the field. *Philos. Trans. Roy. Soc.*, **B273**, 593–610, https://doi.org/10.1098/rstb.1976.0035.

Kirshbaum, D. J., 2011: Cloud-resolving simulations of deep convection over a heated mountain. *J. Atmos. Sci.*, **68**, 361–378, https://doi.org/10.1175/2010JAS3642.1.

Lamraoui, F., J. F. Booth, C. M. Naud, M. P. Jensen, and K. L. Johnson, 2019: The interaction between boundary layer and convection schemes in a WRF simulation of post-cold frontal clouds over the ARM East North Atlantic site. *J. Geophys. Res. Atmos.*, **124**, 4699–4721, https://doi.org/10.1029/2018JD029370.

Langhans, W., J. Schmidli, and C. Schär, 2012: Bulk convergence of cloud-resolving simulations of moist convection over complex terrain. *J. Atmos. Sci.*, **69**, 2207–2228, https://doi.org/10.1175/JAS-D-11-0252.1.

Lv, M., Z. Xu, and Z. L. Yang, 2020: Cloud resolving WRF simulations of precipitation and soil moisture over the central Tibetan Plateau: An assessment of various physics options. *Earth Space Sci.*, **7**, e2019EA000865, https://doi.org/10.1029/2019EA000865.

Ma, N., G.-Y. Niu, Y. Xia, X. Cai, Y. Zhang, Y. Ma, and Y. Fang, 2017: A systematic evaluation of Noah-MP in simulating land-atmosphere energy, water, and carbon exchanges over the continental United States. *J. Geophys. Res. Atmos.*, **122**, 12 245–12 268, https://doi.org/10.1002/2017JD027597.

Manning, J., and R. Baldick, 2019: Forecasting short-term dynamics of shallow cumuli using dynamic mode decomposition. *J. Renew. Sustain. Energy*, **11**, 053704, https://doi.org/10.1063/1.5125927.

Mellor, G. L., and T. Yamada, 1982: Development of a turbulence closure model for geophysical fluid problems. *Rev. Geophys. Space Phys.*, **20**, 851–875, https://doi.org/10.1029/RG020i004p00851.

Miller, S. D., M. A. Rogers, J. M. Haynes, M. Sengupta, and A. K. Heidinger, 2017: Short-term solar irradiance forecasting via satellite/model coupling. *Sol. Energy*, **168**, 102–117, https://doi.org/10.1016/j.solener.2017.11.049.

Milovac, J., K. Warrach-Sagi, A. Behrendt, F. Späth, J. Ingwersen, and V. Wulfmeyer, 2016: Investigation of PBL schemes combining the WRF model simulations with scanning water vapor differential absorption lidar measurements. *J. Geophys. Res. Atmos.*, **121**, 624–649, https://doi.org/10.1002/2015JD023927.

Min, L., D. R. Fitzjarrald, Y. Du, B. E. J. Rose, J. Hong, and Q. Min, 2021: Exploring sources of surface bias in HRRR using New York State Mesonet. *J. Geophys. Res. Atmos.*, **126**, e2021JD034989, https://doi.org/10.1029/2021JD034989.

Min, Q., 2005: Impacts of aerosols and clouds on forest-atmosphere carbon exchange. *J. Geophys. Res.*, **110**, D06203, https://doi.org/10.1029/2004JD004858.

Molod, A., L. Takacs, M. Suarez, J. Bacmeister, I. Song, and A. Eichmann, 2012: The GEOS-5 atmospheric general circulation model: Mean climate and development from MERRA to Fortuna. NASA/TM-2012-104606, Vol. 28, 124 pp., https://gmao.gsfc.nasa.gov/pubs/docs/tm28.pdf.

Nakanishi, M., and H. Niino, 2004: An improved Mellor-Yamada level-3 model with condensation physics: Its design and verification. *Bound.-Layer Meteor.*, **112**, 1–31, https://doi.org/10.1023/B:BOUN.0000020164.04146.98.

——, and ——, 2009: Development of an improved turbulence closure model for the atmospheric boundary layer. *J. Meteor. Soc. Japan*, **87**, 895–912, https://doi.org/10.2151/jmsj.87.895.

Niu, G. Y., and Coauthors, 2011: The community Noah land surface model with multi-parameterization options (Noah-MP): 1. Model description and evaluation with local-scale measurements. *J. Geophys. Res.*, **116**, D12109, https://doi.org/10.1029/2010JD015139.

Olson, J. B., J. S. Kenyon, W. Angevine, J. M. Brown, M. Pagowski, and K. Sušelj, 2019: A description of the MYNN-EDMF scheme and the coupling to other components in WRF-ARW. NOAA Tech. Memo OAR GSD-61, 37 pp., https://doi.org/10.25923/n9wm-be49.

Perez, R., M. David, T. E. Hoff, M. Jamaly, S. Kivalov, J. Kleissl, P. Lauret, and M. Perez, 2016: Spatial and temporal variability of solar energy. *Found. Trends Renew. Energy*, **1**, 1–44, https://doi.org/10.1561/2700000006.

Pielke, R. A., T. J. Lee, J. H. Copeland, J. L. Eastman, C. L. Ziegler, and C. A. Finle, 1997: Use of USGS-provided data to improve climate simulations. *Ecol. Appl.*, **7**, 3–21, https://doi.org/10.1890/1051-0761(1997)007[0003:UOUPDT]2.0.CO;2.

Pleim, J. E., 2007a: A combined local and non-local closure model for the atmospheric boundary layer. Part 1: Model description and testing. *J. Appl. Meteor. Climatol.*, **46**, 1383–1395, https://doi.org/10.1175/JAM2539.1.

——, 2007b: A combined local and nonlocal closure model for the atmospheric boundary layer. Part II: Application and evaluation in a mesoscale meteorological model. *J. Appl. Meteor. Climatol.*, **46**, 1396–1409, https://doi.org/10.1175/JAM2534.1.

Potvin, C. K., and Coauthors, 2020: Assessing systematic impacts of PBL schemes on storm evolution in the NOAA Warn-on-Forecast System. *Mon. Wea. Rev.*, **148**, 2567–2590, https://doi.org/10.1175/MWR-D-19-0389.1.

Rienecker, M. M., and Coauthors, 2008: The GEOS-5 Data Assimilation System—Documentation of versions 5.0.1, 5.1.0, and 5.2.0. Tech. Memo. NASA/TM-2008-104606, Vol. 27, 118 pp., http://gmao.gsfc.nasa.gov/pubs/docs/Rienecker369.pdf.

Schmidli, J., S. Böing, and O. Fuhrer, 2018: Accuracy of simulated diurnal valley winds in the Swiss Alps: Influence of grid resolution, topography filtering, and land surface datasets. *Atmosphere*, **9**, 196, https://doi.org/10.3390/atmos9050196.

Schwitalla, T., O. Branch, and V. Wulfmeyer, 2020: Sensitivity study of the planetary boundary layer and microphysical schemes to the initialization of convection over the Arabian Peninsula. *Quart. J. Roy. Meteor. Soc.*, **146**, 846–869, https://doi.org/10.1002/qj.3711.

Serafin, S., and D. Zardi, 2010: Structure of the atmospheric boundary layer in the vicinity of a developing upslope flow system: A numerical model study. *J. Atmos. Sci.*, **67**, 1171–1185, https://doi.org/10.1175/2009JAS3231.1.

Shin, H. H., and S.-Y. Hong, 2015: Representation of the subgrid-scale turbulent transport in convective boundary layers at gray-zone resolutions. *Mon. Wea. Rev.*, **143**, 250–271, https://doi.org/10.1175/MWR-D-14-00116.1.

Skamarock, W. C., and Coauthors, 2008: A description of the Advanced Research WRF version 3. NCAR Tech. Note NCAR/TN-475+STR, 113 pp., https://doi.org/10.5065/D68S4MVH.

——, and Coauthors, 2019: A description of the Advanced Research WRF Model version 4. NCAR Tech. Note NCAR/TN-556+STR, 145 pp., https://doi.org/10.5065/1dfh-6p97.

Smirnova, T. G., J. M. Brown, S. G. Benjamin, and J. S. Kenyon, 2016: Modifications to the Rapid Update Cycle Land Surface Model (RUC LSM) available in the Weather Research and Forecasting (WRF) Model. *Mon. Wea. Rev.*, **144**, 1851–1865, https://doi.org/10.1175/MWR-D-15-0198.1.

Stull, R. B., 1988: *An Introduction to Boundary Layer Meteorology*. Kluwer, 666 pp.

Taylor, C. M., and R. J. Ellis, 2006: Satellite detection of soil moisture impacts on convection at the mesoscale. *Geophys. Res. Lett.*, **33**, L03404, https://doi.org/10.1029/2005GL025252.

——, D. J. Parker, and P. P. Harris, 2007: An observational case study of mesoscale atmospheric circulations induced by soil moisture. *Geophys. Res. Lett.*, **34**, L15801, https://doi.org/10.1029/2007GL030572.

Thompson, G., and T. Eidhammer, 2014: A study of aerosol impacts on clouds and precipitation development in a large winter cyclone. *J. Atmos. Sci.*, **71**, 3636–3658, https://doi.org/10.1175/JAS-D-13-0305.1.

Trier, S. B., F. Chen, and K. W. Manning, 2004: A study of convection initiation in a mesoscale model using high-resolution land surface initial conditions. *Mon. Wea. Rev.*, **132**, 2954–2976, https://doi.org/10.1175/MWR2839.1.

Wang, J. F., and Coauthors, 2009: Impact of deforestation in the Amazon basin on cloud climatology. *Proc. Natl. Acad. Sci. USA*, **106**, 3670–3674, https://doi.org/10.1073/pnas.0810156106.

Yang, Z. L., and Coauthors, 2011: The community Noah land surface model with multi-parameterization options (Noah-MP): 2. Evaluation over global river basins. *J. Geophys. Res.*, **116**, D12110, https://doi.org/10.1029/2010JD015140.